3rd Specialty Conference on Disaster Prevention and Mitigation
3e Conférence spécialisée sur la prévention et la mitigation des désastres naturels

Montréal, Québec
May 29 to June 1, 2013 / *29 mai au 1 juin 2013*

EXPERIMENTAL STUDY ON THE SEISMIC BEHAVIOUR OF SUSPENDED CEILINGS

Wen-Chun Huang[1], Nahidah Hussainzada[1], and Ghyslaine McClure[1]
[1] Department of Civil Engineering and Applied Mechanics, McGill University, Montreal, QC, Canada

Abstract: Previous earthquakes have exposed the high seismic hazards of suspended ceiling systems (SCSs). Although several researchers have conducted dynamic tests on suspended ceiling systems, most of these studies were focused on their capacity qualification and lacked discussion of their overall seismic behaviour and energy dissipating mechanisms. This study performed shake table tests on 20' x 12' (6.1 m x 3.6 m) suspended ceiling specimens with two groups of seismic inputs obtained from the computed top-floor responses of two Montreal buildings. The purpose of this study was to investigate and discuss the seismic behaviour of SCSs. Two different ceiling types with and without moulding attachment were tested and compared. The first one comprises metal panels with clip-on mechanism to the T-bar supporting grid while the other is with traditional lay-in acoustical panels. The test results revealed that panel movement and drop was localized at the perimeter of the ceiling and that moulding attachments help to retain the ceiling tiles in place and prevent the drop of panels. When the ceiling was attached, plastic deformation of the moulding bracket attachments was observed. For un-restrained SCSs (floating system), damage was observed at the cross runners' connections to the main tees. For this floating system, the energy dissipation mechanism is mainly contributed by the frictional resistance of the various components. Dynamic frictional coefficients ranging from 0.2~0.3 were estimated. The seismic capacity of the tested specimens in this study was evaluated to reach 2.7 g.

1 Introduction

Economic losses and property damage during an earthquake are more often due to the failure of non-structural components than structural members (Taghavi and Miranda, 2003). In many cases, extensive damage of non-structural components interrupts the operations of the building and renders it unusable until repair has been carried out. Suspended ceiling systems (SCSs) are among those non-structural components that may cause significant disruption in the services of a building as they interact with many other functional components located in the ceiling plenum. The use of this type of ceiling has gained in popularity over the past four decades due to its relatively low cost and easy installation. However, following major earthquakes, the seismic vulnerability of SCSs has also been acknowledged. Reported damages range from the drop of panels to total collapse of the ceiling systems (as cited in Gilani et al., 2010; Yao, 2000).

This paper presents the seismic tests performed on a 20' x 12' (6.1 m x 3.6 m) suspended ceiling system. In this study, two types of ceiling panels were used: acoustical lay-in panels (2' x 4' - 0.6 m x 1.2 m and 2' x 2' - 0.6 m x 0.6 m) and metal clip-on panels (2'x2'). The main purpose of the study was to assess the behavior of SCSs and their energy dissipating mechanisms. The ceilings were installed following the ASTM E580M-11 (ASTM International, 2011) guidelines for seismic design categories D, E and F. For comparison purposes, the seismic restraints specified in this standard were removed and was considered as the non-seismic installation. By varying the panel type and the installation parameters, eleven different configurations were tested and compared. The tests were conducted on the earthquake simulator at the Structures Laboratory of École Polytechnique de Montréal in Canada. The seismic motions used in this test were first computed as part of a study on the seismic performance of partition walls (Huang et al., 2009). The results presented include the seismic performance of the acoustic lay-in panels and the metal clip-on panels, their energy dissipating mechanism as well as their seismic capacity.

2 Experimental Study

2.1 Testing Setup

The earthquake simulator at the Structures Laboratory of École Polytechnique de Montréal was used to perform seismic tests on a 20’x12’ (6mx3.6m) ceiling with a plenum height of 2’ (0.6m). The simulator is unidirectional and measures 3.4m x 3.4m. The operating frequency of the shake table ranges up to 50 Hz. Its operating displacement, velocity and acceleration are of ±125 mm, ±800 mm/s and ±3g, respectively. A steel frame extension platform of dimensions 22 ’x 14’ x 10.8’ (6.7 m x 4.3 m x 3.3 m) was constructed to support the full-scaled ceiling specimens. A bulkhead hanging wall made of plywood and metal studs was used to simulate a realistic bulkhead wall. The ceiling moulding was screwed to the hanging wall. Figure 1 shows a 3D view of the platform and installed specimen as well as a close-up on an installed 2’x2’ acoustical ceiling specimen.

(a) Sketch of testing set-up (b) Complete test installation (c) Ceiling Specimen with 2’x2’ panels

Figure 1 Testing Platform and Hanging Wall with Ceiling Specimen

2.2 Testing Configurations

Three main installation configurations as shown in Figure 2 were tested: (a) seismic, (b) non-seismic with moulding attachment, (c) non-seismic without moulding attachment. Furthermore, besides the standard acoustical lay-in tiles (2’x4’ and 2’x2’), the metal clip-on butt-edge panels (2’x2) equipped with a clip that restrains them from falling were also tested, as shown in Figure 2(d).

Requirements meeting those stated for seismic design categories D, E and F in ASTM E580M-11b (ASTM International, 2011) were considered as seismic installation. Some of the key features of the seismic installation are illustrated in from Figure 3(a) to Figure 3(f), including: (a) the support ledge of the wall moulding must be of at least two-inch long and a gap of ¾ of an inch should be held, (b) the main tees must be attached to the wall on two adjacent sides, (c) the main runners must be suspended at a spacing of 48 inch, (d) at the perimeter of the ceiling, the cross and the main runners must be hung at a maximum distance of 8 inch from the walls, (e) stabilizer bars must be used within 24 inch of the walls at the two floating edges to prevent the spread of the cross-tees, and (f) the hanger wires must be wrapped at least three times within a length of three inches and must not be more than 1/6 inch out of plumb.

The grids of ceiling specimens were installed in two directions: in the longitudinal direction with the main runners parallel to the acceleration input while in the transverse direction with the main tees perpendicular to the seismic motion. Figure 4 shows the layouts and joints of the main runners and the direction of the seismic input. By varying the ceiling panel type, the installation parameters and the direction of seismic loading, eleven different configurations were tested as listed in Table 1.

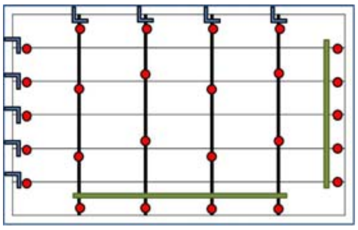

(a) Seismic installation

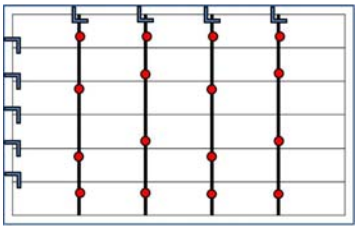

(b) Non-seismic installation with moulding attachment

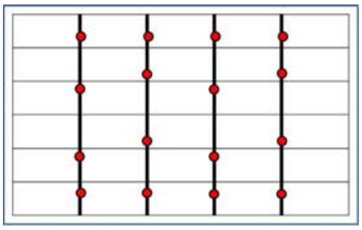

(c) Non-seismic installation

(d) Metal panels with the clip-on mechanism

Figure 2 Configurations of the tested ceiling specimens with/without seismic installation

(a) 2” Wall Moulding and ¾” Gap

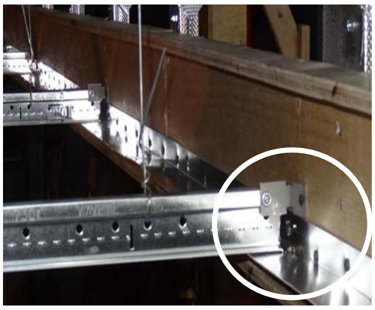

(b) Moulding Attachment

(c) Interior Wire Spacing

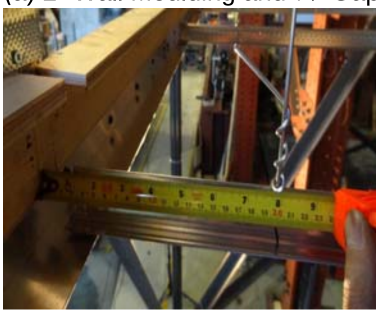

(d) Perimeter Wire

(e) Stabilizer Bars

(f) Slope of Hanger Wire

Figure 3 Seismic requirements as per ASTM E580M-11b

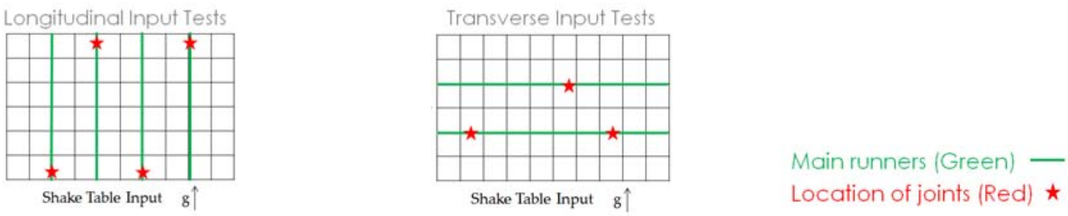

Figure 4 Configurations of longitudinal and transverse seismic inputs

Table 1 Summary of the tested SCS configurations

SCS Configuration	Moulding Attachment	Gap (in)	Stabilizer Bars	Perimeter Hanger Wires on all Tees	Loading Direction
ASC_2'X4'_S_A	Yes	¾	Yes	Yes	Longitudinal
ASC_2'X4'_NS_A	Yes	-	No	No	
ASC_2'X4'_NS_NA	No	-	No	No	
ASC_2'X2'_NS_NA	No	-	No	No	
MCP_2'X2'_S_A	Yes	¾	Yes	Yes	
MCP_2'X2'_NS_A	Yes	-	No	No	
MCP_2'X2'_NS_NA	No	-	No	No	
MCP_2'X2'_S_A_T	Yes	¾	Yes	Yes	Transverse
MCP_2'X2'_NS_NA_T	No	-	No	No	
ASC_2'X2'_NS_NA_T	No	-	No	No	
ASC_2'X4'_NS_NA_T	No	-	No	No	

Notes:
*ASC_2'X4'_S_A: Acoustic Suspension Ceiling _2'x4' Panels_Seismic Installation_with Attachment
MCP_2'X2'_NS_NA_T: Metal Clip-on Panel_2'x2' Panels_Non-Seismic Installation_No Attachment_Transverse Loading
**No special requirements exist for the required gaps at runner ends for non-seismic installation

2.3 Seismic Input

The seismic inputs used in this study are listed in Table 2. Two Montreal office buildings: a 27-storey building (Building A) and a 14-storey building (Building B) were simulated in SAP2000. Seismic motions that match the Montreal and Vancouver response spectra were used to obtain the top floor accelerations for 10% and 2% probability of exceedance in 50 years. The computed top floor responses were then used as the seismic input in this study. Further details about the seismic motions can be found in Huang et al., 2009, Atkinson and Beresnev, 1998, and Filiatrault et al., 2004.

Table 2 Seismic Input and Target Peak Acceleration

Input Sequence	Seismic Event	Target Peak (g)
1	A_M10%_E70_300	0.11
2	B_M10%_E70_200	0.26
3	A_V10%_W72_100	0.29
4	B_V10%_W60_50	0.53
5	A_Chichi_T76_50	0.42
6	B_Chichi_T76_50	0.43
7	A_M2%_E70_100	0.53
8	A_V2%_W72_70	0.49
9	B_M2%_E70_70	0.76
10	B_V2%_W65_50	1.01
11	A_Chichi_T76_15	1.45

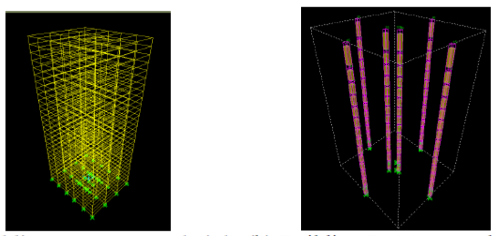

(a) Building A, 27-storey height T= 2.71s (b) Building B, 14-storey height T= 0.71s

Notes*:
- A_M10%_E70_300: Top floor acceleration response of Building A under Eastern earthquake input with magnitude 7.0 at 300 km from the epicenter.
- A and B indicates top floor response of Building A and Building B, respectively.
- M: Montréal; V: Vancouver
- %: Percentage probability of exceedance in 50 years

2.4 Instrumentation

A schematic outline of the instrumentation used in the tests is shown in Figure 5. The accelerometers were placed on the four main runners of the ceiling grid and both the longitudinal and transverse motions were monitored. The displacement meters measured the relative distance between the ceiling grid and the bulkhead wall. Instruments were also placed on the platform floor to assess the acceleration frequency transfer function between the ceiling and the platform floor.

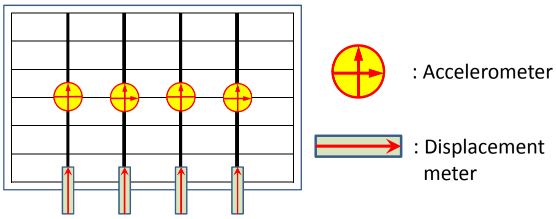

Figure 5 Instrumentation of Ceiling Grid

3 Testing Results

3.1 Damage Modes of SCSs

The performance of the SCSs was assessed based upon both the responses of the panels and grids. In terms of the panels, three distinctions were made: panel movement (PM) followed by dislocation (PD), and finally, panel fall (PF) as shown in Figure 6. For the suspension grid system, plastic deformation of the brackets occurred, as shown in Figure 7(a), during the strongest seismic input motion for the SCS specimens with the moulding attachments. When no attachment was provided, some cross runners at the perimeter were observed to slip and get stuck to the moulding angle, due to the achieved displacement of the ceiling system exceeding the moulding length, as shown in Figure 7(b). In Figure 7(c), joint damages of cross-runners have been observed. Noteworthily, no grid damage was observed for the SCSs with metal panels.

(a) Panel Movement (PM) (b) Panel Dislocation (PD) (c) Panel Fall (PF)

Figure 6 Failure modes of the acoustic panels

(a) Bracket Deformation (BD) (b) Grid Stuck to Moulding (GS) (c) Grid Damage (GD)

Figure 7 Damage patterns of the suspension grid system

A summary of the testing results is presented in Table 3. For all eleven configurations, panel failure (panel moved, dislocated or fell down) was only observed at the perimeter of the ceiling. When comparing the acoustic and the metal panels, it was observed that the onset of panel movement occurred earlier for the acoustic panel. Moreover, a larger number of panel failures are noted for the acoustic tiles compared to the metal tiles due to their butt-edge characteristics, which restrained panel movement. For the ceiling configurations installed as per the ASTM E580M-11b recommendations (seismic installation), fewer panel movements and dislocations were recorded and no loss of panels occurred. Panel fall was only observed for ASC_2’X4’_NS_WA and ASC_2’X4’_NS_WA systems with one and three dropped tiles, respectively. No panel fall was observed for the metal panels due to their clip-on mechanism. Briefly concluding, PM and PD occurred to all of the SCSs, while the PF occurred only to the non-seismic SCSs with the lay-in acoustic panels.

When comparing the longitudinal with the transverse seismic loading inputs, fewer panel movements and no panel drop occurred for the transverse loading direction. This is because when the seismic load was applied transversely (perpendicular to main runners), the movement of the cross-tees was restricted by the main-tees, which are continuous. However, when the seismic input was along the main runners, the restraint ability of the non-continuous 2’ or 4’ cross-runners were less, thus more panel movements were observed.

Table 3 Summary of the testing results

Seismic Event	**APA (g)**	**Longitudinal Loading**							**Transverse Loading**			
		ASC 2’X4’ S	**ASC 2’X4’ NS_A**	**ASC 2’X4’ NS_ NA**	**ASC 2’X2’ NS_ NA**	**MCP 2’X2’ S_A**	**MCP 2’X2’ NS_A**	**MCP 2’X2’ NS_ NA**	**MCP 2’X2’ S_A_ T**	**MCP 2’X2’ NS_A_ T**	**ASC 2’X2’ NS_ NA_T**	**ASC 2’X4’ NS_ NA_T**
A_M10%_ E70300	0.15	-	-	-	-	-	-	-	-	-	-	-
B_M10%_ E70200	0.25	-	-	-	3 PM	-	-	-	-	-	-	-
A_V10%_ W72100	0.29	-	-	-	4 PM	-	-	-	-	-	-	-
B_V10%_ W6050	0.79	3 PM	3 PM	4 PM	3 PM	-	-	2 PM	-	6 PM	-	-
A_ChiChi_ T7650	0.53	-	2 PM	2 PM	2 PM	-	-	2 PM	-	-	1 PM	-
B_ChiChi_ T7650	0.46	-	2 PM	4 PM	2 PM	-	-	3 PM	-	-	1 PM	-
A_M2%_ E70100	0.49	-	-	5 PM	3 PM	-	-	2 PM	-	-	1 PM	-
A_V2% _W7270	0.49	-	-	5 PM	2 PM	-	-	2 PM	-	-	1 PM	-
B_M2%_ E7070	0.90	9 PM 1 PD	13PM	5 PM	3 PM	4PM	2 PM	4 PM	-	14 PM	4 PM	4 PM
B_V2%_ W6550	1.26	10PM 2 PD	11PM 1 PD	3 PM 1 PD	PM 3 GS	4PM	2 PM	3 PM 1 PD	-	20PM	6 PM	4 PM 1 PD
A_ChiChi_ T7615	2.63	11PM 2 PD BD	11PM 1 PD 1 PF BD	7 PM 4 PD 3 PF GD	12PM GS 1GD	7PM	7 PM	3 PD	-	20PM 1 PD	6 PM GS	4 PM 2 PD 2 GS

Notes*:
ASC_2’X4’_S_A: Acoustic Suspension Ceiling _2’x4’ Panels_Seismic Installation_with Attachment
MCP_2’X2’_NS_NA_T: Metal Clip-on Panel_2’x2’ Panels_Non-Seismic Installation_No Attachment_Transverse Loading
APA (g): an average of the achieved peak acceleration (APA) of the platform was calculated for all ceiling configurations
PM= panel movement, PD= panel dislocation, PF=panel fall.
BD= damage to brackets, GS= grid stuck to moulding, GD= grid damage

3.2 Dynamic Behaviour of SCSs

When considering the dynamic behaviour of the SCSs, the ceiling systems were classified into two distinct categories: attached (with moulding bracket attachment) and floating (without moulding bracket attachment) systems. In this study, two acceleration transfer functions (output/input) in the frequency domain of some selected SCSs were calculated and compared, as shown in Figure 8, to investigate their dynamic characteristics. One of the calculated transfer functions is ceiling-grid/platform-floor and the other is hanging-wall/platform-floor.

For the attached system (MCP_2'X2'_S_A), the transfer function reveals that the bulkhead hanging wall and the ceiling grids behaved similarly. The natural frequency for this system (wall and grid) is measured to be around 16 Hz, as shown in Figure 8(a), under the small excitations. When the seismic input rises to higher amplitude (A_ChiChi_T7615), the wider bandwidth of the transfer function curves is observed in Figure 8(b), indicating the damping of the system has been increased. This is due to the plastic deformation of the moulding attached brackets under violent shaking. Overall, the ceiling grids and the bulkhead hanging wall still behaved as one system.

For the floating system (ASC_2’X2’_NS_NA), the walls and the ceiling grids also behaved as one system at the beginning, until the grids started to slip. From the transfer function in Figure 8(c), it is seen that the grids and the hanging bulkhead wall acted as one system under small excitation (A_M10%_E70_300), and the natural frequency of the first mode was 16 Hz. Once the slip occurred under the larger seismic event (A_M2%_E70_100), the grids behaved independently and the fundamental natural frequency shifted to 7 Hz, as shown in Figure 8(d). From the results, it is observed that the floating SCSs act as a nonlinear system, depending on the input acceleration magnitude and the sliding friction may play an important role to dissipate energy.

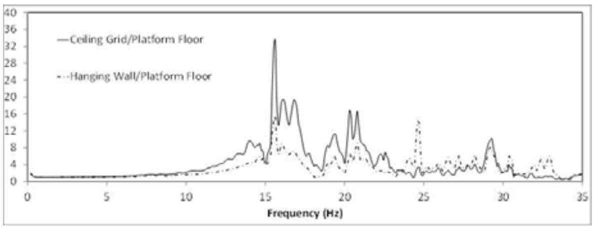

(a) B_V10%_W60_50 input to MCP_2'X2'_S_A

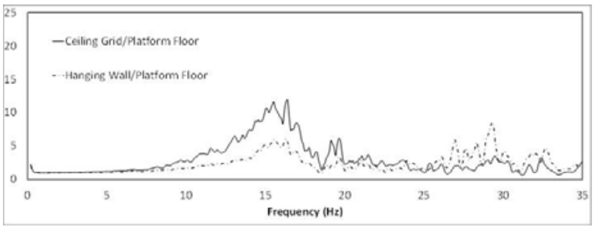

(b) A_ChiChi_T76_15 input to MCP_2'X2'_S_A

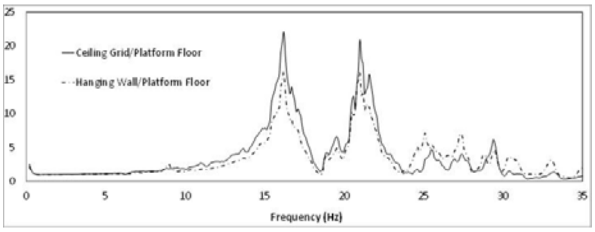

(c) A_M10%_E70_300 input to ASC_2’X2’_NS_NA

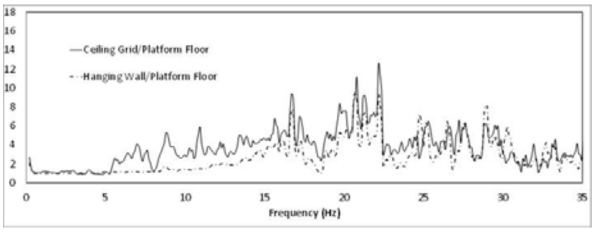

(d) A_M2%_E70_100 input to ASC_2’X2’_NS_NA

Figure 8 Comparison of the transfer functions between attached and floating SCSs

In dynamic systems, the hysteresis loops are plotted using the sum of the spring force and the damping force versus the displacement of the system, and they are often used to assess the damping property of the system. Also, from the equation of motion of a linear single degree-of-freedom (SDOF) system, the inertial force (mass*acceleration) acts in the opposite direction of the resultant of the spring force, damping force and the external load. Therefore, in order to observe the energy dissipating mechanism, plots of the acceleration vs. displacement responses of the tested SCSs are shown in Figure 9. For the attached SCSs in Figures 9(a) and 9(b), the hysteresis loops contained linear trends, which indicates the influence of the stiffness contributed by the moulding attachment brackets. For comparison, the hysteresis loops of the floating SCSs shown in Figures 9(c) and 9(d) reveal that the stiffness vanished with the removal of the moulding attachment brackets, resulting in flat hysteresis loops which characterize Coulomb frictional damping. Therefore, based upon the investigation, it is concluded that the energy dissipating mechanism for the floating SCSs was mainly provided by the frictional resistance of the system. A simplified conceptual SDOF model could be further established as shown in Figure 10(a).

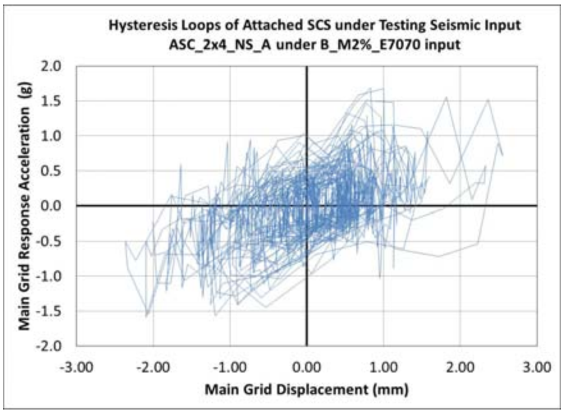

(a)

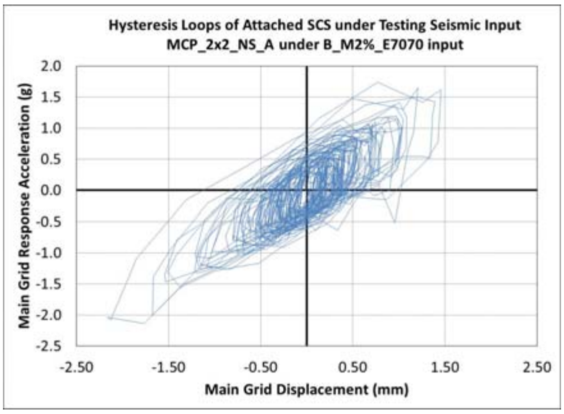

(b)

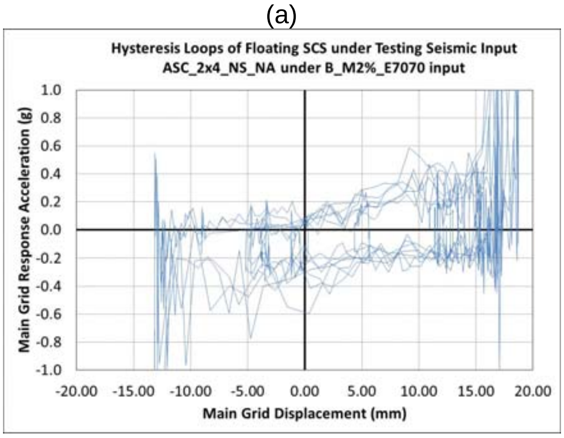

(c)

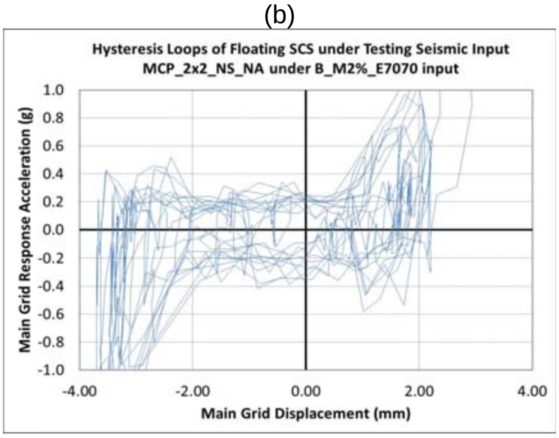

(d)

Figure 9 Hysteresis loops of SCSs under seismic inputs

In Figure 10, the mass ‘m’ represents the mass inertia of the SCS, including panels and runners, suspended by a wire with an initial Gap from the wall mouldings. The lateral stiffness of the system is represented by ‘k’. The coefficient of friction (dynamic) is represented by ‘μ’ and the inherent damping by ‘c’. While the system slides and the gap is open (see Figure 10 (a)), the frictional force (μ*m*g) is equal to the inertia force (m*a, where ‘a’ represents the response acceleration of the SCSs), since no other force is present in the system. Thus, from curves of the response acceleration vs. displacement, the frictional coefficients could be determined. By observing the response acceleration of the floating SCSs before hitting the moulding perimeters in Figures 9(c) and 9(d), the dynamic frictional coefficients were estimated to be ranging from 0.2~0.3. Once the frictional coefficient was determined, the numerical model of the attached SCSs could be further simulated in Figure 10(b) by removing the Gap. The stiffness of the tested SCSs could be obtained by applying the curve fitting technique to the trended hysteresis loops shown in Figures 9(a) and 9(b).

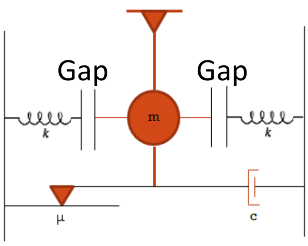

(a) Floating SCS

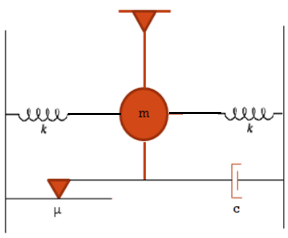

(b) Attached SCS

Figure 10 Simplified Conceptual SDOF Model of the SCSs

4 Discussion

4.1 Seismic Capacity of SCSs

It is difficult to assess the seismic capacity of the SCSs tested in this study as no major damage was observed during the tests. As well, different ceiling configurations achieved different peak acceleration levels at the ceiling grids, thus determining the seismic capacity for a panel type is not straightforward. Two criteria may be used to evaluate the seismic capacity: the failure of the grid or the loss of ceiling panels. In terms of the failure of the grid system and their connection joints, the seismic capacity of the tested SCSs in this study could reach 2.7g. This value is the lowest mean value of APA of the ceiling grid above which some damage to the cross runners connection joints was observed. Panel loss could also represent a critical issue depending on the occupancy and the importance of buildings. The loss of ceiling panels represents a falling debris hazard for occupants and may also be harmful to sensitive and expensive equipment in post-disaster buildings such as hospitals. When comparing the performance of the two panel types studied, the metal clip-on panels performed better than the acoustic panels as they experienced no panel drop nor suffered any damage to the grid system. This may be explained by the butt-edge characteristics of this panel type which restrains panel movement as well as the clip-on mechanism which prevents the tile from detaching from the supporting grid.

4.2 Seismic and Non-Seismic Installations

As indicated in Table 3, the SCSs installed according to the ASTM E580M-11b standard were observed to perform better than the non-seismic installations, for more panel movements and panel fall were observed for the latter system. The attached SCSs also performed better than the floating system as the bracket moulding attachments helped in maintaining the ceiling panels in place to prevent large relative motion between the ceiling grid and the wall.

5 Conclusion

In this study, eleven 20'x12' suspended ceiling systems were tested on a unidirectional seismic simulator, with parameters including various installation details, ceiling panel types, and seismic input directions. The input seismic motions were obtained from the calculated top floor response of two Montreal buildings subjected to eleven seismic events. The main findings of this study are as follows:

1. Panel loss was localized at the perimeter of the tested SCSs. The metal clip-on panels experienced less panel movement due to their butt-edge characteristic, and their clip-on mechanism prevented the panels from dropping.

2. For seismic installation, plastic deformation of the moulding attachment brackets was observed after strong shaking. The brackets helped to maintain the ceiling panels in place. For non-seismic installation, besides panel falling, damages also occurred at the joints between cross runners and the main tees. The seismic capacity of all of the tested SCSs could reach 2.7g in terms of the onset of damage to the ceiling grid.

3. The energy dissipation mechanism of the floating SCSs is mainly contributed by friction. The frictional coefficients ranging from 0.2~0.3 were observed and estimated.

Acknowledgements

The seismic tests were conducted at the Structures Laboratory of École Polytechnique de Montréal with the assistance of testing engineer Martin Leclerc. The ceiling materials were provided by Armstrong/Simplex Ceilings of Montréal and the support of Mr. Michel Desjardins is greatly acknowledged. This research was funded by Strategic Research Project Grant STPGP 396464 from the Natural Sciences and Engineering Research Council of Canada, and by *Fonds Québécois pour la recherche Nature et*

Technologie (FQRNT), regroupement stratégique CEISCE, Centre d'études interuniversitaire sur les structures sous charges extremes.

References

ASTM International, 2011. Standard Practice for Application of Ceiling Suspension Systems for Acoustical Tile and Lay-in Panels in Areas Subject to Earthquake Ground Motions. ASTM E580M-11, ASTM International, West Conshohocken, PA, USA.

Atkinson, G.M., and I. A. Beresnev, 1998. Compatible ground-motion time histories for new national seismic hazard maps, Can. J. of Civil Engrg. 25(2): 305-318.

Badillo-Almaraz, H., Whittaker, A. S., Reinhorn, A. M., and Cimellaro, G. P., 2006. Seismic fragility ofsuspended ceiling systems. Multidisciplinary Center for Earthquake Engineering Research, Univ. at Buffalo–State Univ. of New York (SUNY), Buffalo, N.Y., USA.

Filiatrault, A., R. Tremblay, and S. Kuan, 2004. Generation of floor accelerations for seismic testing of operational and functional building components, Can. J. of Civil Engrg. 31(4): 646-663.

Gilani, ASJ, Reinhorn, AM, Glasgow, B, Lavan, O, and Miyamoto, HK, 2010. Earthquake simulator testing and seismic evaluation of suspended ceilings. ASCE/J Archit. Eng 16(2):63–73.

Huang, W-C., McClure, G. and Yao, G.C., 2010. Shake Table Testing on Moveable Office Partitions without Top Restraint. *Proc. 9th US National and 10th Can. Conf. on Earthquake Engineering: Reaching Beyond Borders*, EERI and CAEE, 25-29 July, Paper 963, 10 p.

Rihal, S. and Granneman, G.,1984. Experimental Investigation of the Dynamic Behavior of Building Partitions and Suspended Ceilings during Earthquakes. Report No. ARCE R84-1,California Polytechnic State University, Pomona, CA, USA.

Taghavi, S., and Miranda, E., 2003. Response assessment of nonstructural building elements. PEER report2003/05,College of Engineering, University of California Berkeley, CA, USA

Yao, G. C., 2000. Seismic Performance of Direct Hung Suspended Ceiling Systems. Journal of Architectural Engineering, 6(1): 6-11.